THE JOURNAL OF BIOLOGICAL CHEMISTRY
Vol. 278, No. 47, Issue of November 21, pp. 46734–46740, 2003

Printed in U.S.A.

Different Interaction Modes of Two Cytochrome-*c* Oxidase Soluble Cu_A Fragments with Their Substrates*

Received for publication, July 15, 2003, and in revised form, August 22, 2003
Published, JBC Papers in Press, August 23, 2003, DOI 10.1074/jbc.M307594200

Oliver Maneg‡, Bernd Ludwig‡, and Francesco Malatesta§¶

From ‡Molekulare Genetik, Biozentrum, J. W. Goethe-Universität, Marie-Curie-Str. 9, Frankfurt D-60439, Germany and §Dipartimento di Biologia di Base ed Applicata, University of L'Aquila, via Vetoio, loc. Coppito, L'Aquila I-67010, Italy

Cytochrome-*c* oxidase is the terminal enzyme in the respiratory chains of mitochondria and many bacteria and catalyzes the formation of water by reduction of dioxygen. The first step in the cytochrome oxidase reaction is the bimolecular electron transfer from cytochrome *c* to the homobinuclear mixed-valence Cu_A center of subunit II. In *Thermus thermophilus* a soluble cytochrome c_{552} acts as the electron donor to ba_3 cytochrome-*c* oxidase, an interaction believed to be mainly hydrophobic. In *Paracoccus denitrificans*, electrostatic interactions appear to play a major role in the electron transfer process from the membrane-spanning cytochrome c_{552}. In the present study, soluble fragments of the Cu_A domains and their respective cytochrome *c* electron donors were analyzed by stopped-flow spectroscopy to further characterize the interaction modes. The forward and the reverse electron transfer reactions were studied as a function of ionic strength and temperature, in all cases yielding monoexponential time-dependent reaction profiles in either direction. From the apparent second-order rate constants, equilibrium constants were calculated, with values of 4.8 and of 0.19, for the *T. thermophilus* and *P. denitrificans* c_{552} and Cu_A couples, respectively. Ionic strength strongly affects the electron transfer reaction in *P. denitrificans* indicating that about five charges on the protein interfaces control the interaction, when analyzed according to the Brønsted equation, whereas in the *T. thermophilus* only 0.5 charges are involved. Overall the results indicate that the soluble Cu_A domains are excellent models for the initial electron transfer processes in cytochrome-*c* oxidases.

The aerobic electron transport chain of *Paracoccus denitrificans* represents a model system for the mitochondrial respiratory chain, where the terminal reaction, the reduction of dioxygen to water, is mediated by cytochrome-*c* oxidase (EC 1.9.3.1). The electrons for this reaction are donated by a *c*-type cytochrome (7) and enter the oxidase via the Cu_A center (for a recent review see Ref. 2), a highly conserved motif in subunit II of cytochrome-*c* oxidases of eukaryotes, aerobic bacteria, and in the nitrous oxide reductase of denitrifying bacteria. The Cu_A center resides in a periplasmic, solvent-exposed domain of subunit II and contains two copper ions in a mixed valence state, which give rise to the typical purple color of the isolated domain (3). The two copper atoms are bound by two cysteine residues forming thiolate bridges, two histidine residues, and as further ligands a methionine sulfur and a glutamate peptide carbonyl. Soluble domains of several bacterial cytochrome-*c* oxidases have been prepared including *P. denitrificans* (3), *T. thermophilus* (4), *Paracoccus versutus* (5), and *Bacillus subtilis* (6). Following electron transfer to the Cu_A center from cytochrome *c*, electrons are further transferred to the low-spin heme *a* (or *b*) in subunit I, in a very fast μs time-scale process, and finally to the binuclear heme a_3-Cu_B site (on a ms time scale), where dioxygen is reduced to water. In *P. denitrificans* two *c*-type cytochromes have been suggested to mediate the ET[1] processes between the bc_1 complex and the terminal electron accepting enzymes, the aa_3- and the cbb_3-type cytochrome-*c* oxidases, and the nitrite and the nitrous oxide reductases of the nitrate respiratory pathway. A soluble cytochrome c_{550} is believed to function as an electron donor in different respiratory pathways such as in methanol and methylamine oxidation or in denitrification (7). The kinetics of the electron transfer reaction between this cytochrome and a soluble Cu_A domain from *P. denitrificans* aa_3 cytochrome-*c* oxidase have been studied (8). However, there is ample evidence that a different cytochrome, cytochrome c_{552}, is the genuine mediator between the bc_1 complex and aa_3. This 18-kDa cytochrome (9) is composed of three functional domains: an N-terminal helical membrane anchor, a negatively charged spacer region, and a typical class I *c*-type heme domain. This cytochrome is believed to be the *bona fide* electron transfer shuttle protein between the bc_1 complex and aa_3, because (i) a ternary supercomplex consisting of these three components is isolated under certain detergent solubilization conditions from *P. denitrificans* membranes (10); (ii) electron transport from NADH to dioxygen in isolated membranes is blocked in deletion mutants lacking the c_{552}-coding gene, but this inhibition may be overcome by mitochondrial cytochrome *c* (11), and (iii) specific antibodies directed against purified cytochrome c_{552} can block electron transport from NADH to oxygen in membrane activity assays (9).

At low ionic strength (*i.e.* below 10 mM), the reaction between mitochondrial cytochrome *c* and cytochrome-*c* oxidase involves the formation of a 1:1 stoichiometric complex, which may be isolated *in vitro* (12). Under these conditions, complex formation is believed to rate-limit the subsequent rapid intracomplex

* This work was supported in part by Deutsche Forschungsgemeinschaft Grant SFB 472 and Fonds der Chemischen Industrie (to B. L.), by Deutscher Akademischer Austauschdienst and Conferenza dei Rettori delle Università Italiane Vigoni Program (to B. L. and F. M.), and by a Programma di Ricerca Scientifica Interuniversitario Nazionale "Bioenergetica: Aspetti Genetici, Biochimici e Fisiopatologici" from the Ministero dell'Istruzione, dell'Universita' e della Ricerca of Italy (to F. M.). The costs of publication of this article were defrayed in part by the payment of page charges. This article must therefore be hereby marked "*advertisement*" in accordance with 18 U.S.C. Section 1734 solely to indicate this fact.

¶ To whom correspondence should be addressed. Tel. 39-0862433287; Fax: 39-0862433273; E-mail: malatest@univaq.it.

[1] The abbreviations used are: ET, electron transfer; TEV, tobacco etch virus.

ET process (13). From the strong ionic strength dependence of the reaction and from mutagenesis studies (14, 15) a two-step model has been proposed for the interaction of the proteins. Initially the orientation is mediated by long range electrostatic forces, followed by the fine-tuning of the interaction by hydrophobic patches within the docking site. In contrast to this, nearly no charged residues are found on the probable interaction interfaces of the corresponding proteins from *T. thermophilus*, as demonstrated by the recently solved crystal structures of the ba_3 cytochrome-*c* oxidase (16) and its substrate (17), a soluble cytochrome spectroscopically identified as c_{552} (18). *T. thermophilus* is a Gram-negative, extremely thermophilic eubacterium found in hot springs with optimum growth temperature around 75 °C. Taking into consideration that the stability of electrostatic interactions is lower at higher temperatures, hydrophobic interactions become more favorable. Kinetic studies have shown that the turnover activity of cytochrome c_{552} with ba_3 oxidase becomes faster as ionic strength is decreased (19). On the contrary, *P. denitrificans* aa_3 cytochrome-*c* oxidase shows very low turnover rates under low ionic strength conditions, most likely because of the formation of a high affinity electrostatic complex (15). Elucidation of the cytochrome *c*-Cu_A electron transfer mechanism is complicated by the subsequent monomolecular ET events taking place along the reaction coordinate that complete the reduction of dioxygen to water. It was, therefore, of interest to isolate and compare both periplasmically oriented subunit II Cu_A domains from *P. denitrificans* and *T. thermophilus* and to study the electron transfer reactions with their cytochrome c_{552} electron donor counterparts. Differences between the two systems with respect to the relevant electron transfer reactions can be studied directly by stopped-flow spectroscopy without interference from heme *a* absorbance and by the subsequent electron transfer and energy transduction events. The results indicate that the expressed soluble Cu_A domains are excellent models for the initial electron transfer events in cytochrome-*c* oxidases.

EXPERIMENTAL PROCEDURES

Expression and Purification Procedures—Expression of the Cu_A fragment of *P. denitrificans* subunit II, encoded by the *cta*C gene (20), was carried out in *Escherichia coli* JM 109. The region representing amino acid residues 130–280 of the Cu_A domain was amplified by PCR. The subunit II-BamHI-TEV primer with sequence act*gggatcc*g*aaaacctatact-tccaaagc*caggagatgccgaacg (BamHI site underlined, TEV site in italics) was used as forward primer, coding for the TEV-protease recognition site (ENLYFQS, with cleavage between Q and S). As a reverse primer an oligonucleotide was used according to Lappalainen *et al.* (3), introducing a HindIII site, to allow for cloning into the expression vector pQE-30 (Qiagen). This construct provides considerably higher expression rates (up to 8 mg/liter) than the previous method (3). Because the His tag (coded on the parent vector) is not used for purification, nor is its presence in the protein desirable, it was cleaved off *in vivo* by co-transforming pRK603 into this *E. coli* strain (21), thus providing constitutive expression of the TEV-protease. Cells were grown on minimal medium containing 40 g/liter glycerol, 7.5 g/liter K_2HPO_4, 5.3 g/liter NaH_2PO_4-H_20, 2 g/liter NH_4Cl, 1 g/liter glucose, 1 mM $MgSO_4$, 0.1 mM $CaCl_2$, 10 ml/liter trace element solution 1 (22), 0.2 μM thiamin, 100 μg/ml ampicillin, 25 μg/ml kanamycin, in a 10-liter New Brunswick Microferm fermentor. Cells were induced with 0.2 mM isopropyl-1-thio-β-D-galactopyranoside at an A_{600} of ~4.0. After 4 h cells were harvested, and preparation of inclusion bodies, protein refolding, copper insertion, and purification were carried out essentially as described previously (3). Gel filtration was done on Sephacryl HR S200 (Amersham Biosciences), and an additional purification step on a nickel-nitrilotriacetic acid column (Qiagen) in 20 mM Bis-Tris buffer at pH 7.0 removed residual His-tagged material, as determined by SDS-PAGE (not shown).

The Cu_A fragment of the *T. thermophilus* ba_3 cytochrome-*c* oxidase was expressed and purified as described previously (4). The cytochrome c_{552} soluble domain of *P. denitrificans* was expressed in *E. coli* according to the published protocol (23). Following a similar approach, the *T. thermophilus* cytochrome c_{552} gene was cloned into pET22b, a vector providing the *pel*B leader, which directs the protein to the periplasm. Correct assembly and insertion of the cofactor into the apoprotein was achieved by cotransforming *E. coli* cells with the heme maturation plasmid pEC86 (24). Purification was carried out according to Fee *et al.* (25). Protein concentration was determined by using the following extinction coefficients: Pd-c_{552} $\Delta\epsilon_{\text{Red-Ox, 552 nm}}$ = 19.4 mM^{-1} cm^{-1}, Pd-Cu_A $\epsilon_{480\text{ nm}}$ = 3.0 mM^{-1} cm^{-1}, Tt-c_{552} $\Delta\epsilon_{\text{Red-Ox, 552 nm}}$ = 21.0 mM^{-1} cm^{-1}, Tt-Cu_A $\epsilon_{530\text{ nm}}$ = 3.1 mM^{-1} cm^{-1}.

Stopped-flow Spectroscopy and Experimental Protocol—Kinetic experiments were carried out by using a thermostatted Applied Photophysics stopped-flow apparatus (Leatherhead, United Kingdom) with a 1-cm observation chamber. The ET kinetics between the soluble Cu_A domains and cytochromes *c* were studied in both the forward (physiological) and reverse directions according to the following experimental protocol (Scheme 1), which was devised to (i) minimize the auto-oxidizability of the reduced proteins, and to (ii) better control the initial absolute concentration of the reduced proteins. According to Scheme 1,

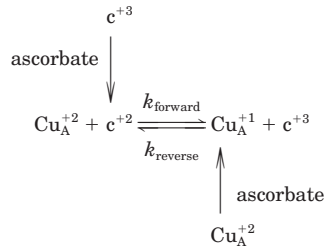

SCHEME 1

one of the partner proteins is initially reduced anaerobically in the stopped-flow syringe by ascorbate (see *vertical arrows*), which at the chosen solution pH is a slow reductant (see below). Following complete reduction, the solution is mixed in the stopped-flow apparatus with an anaerobic solution containing the oxidized ET acceptor protein, and the time-dependent extinction changes followed at 551 nm (*P. denitrificans*) or at 552 nm (*T. thermophilus*). Thus, in the forward direction cytochrome *c* is reduced by ascorbate and mixed with oxidized Cu_A, whereas in the reverse direction prereduced Cu_A is mixed with oxidized cytochrome *c*. In all experiments the buffer (20 mM Bis-Tris, pH 7.0, with ionic strength varied by appropriate amounts of KCl) was flushed with N_2 in a glass gas-tight syringe (fitting the stopped-flow valve) for at least 15 min, and following addition of the protein of interest, the solution was flushed for an additional 15 min. Finally 0.5 mM sodium ascorbate was added from a 1.0 M stock solution. All experiments were performed at 8 °C.

Complete reduction was achieved after several minutes, as determined separately in stopped-flow experiments in which sodium ascorbate, at varying pseudo-first order concentrations, was mixed with either oxidized protein (see Fig. 1 and "Results and Discussion"). The apparent bimolecular rate constants for reduction of the Cu_A domains both from *P. denitrificans* and *T. thermophilus* and the corresponding soluble cytochromes c_{552} were in the range of 60 to 330 M^{-1} s^{-1} (results not shown), 3–5 orders of magnitude smaller than the ET process of interest.

Under all the experimental conditions tested (cytochrome *c* concentration, ionic strength, and temperature), the forward and reverse ET apparent bimolecular rate constants were determined by fitting the observed kinetic traces to a simple exponential relaxation process at different ferro- or ferricytochrome *c* concentrations (forward and reverse directions, respectively) followed by linear regression of the observed rate constants to the varied cytochrome *c* concentrations. Three or more kinetic traces were acquired for each specific experimental condition and averaged. True pseudo-first order conditions could not be completely achieved throughout the kinetic titration experiments because of the high cytochrome *c* (19.4–21.0 mM^{-1} cm^{-1}) and low Cu_A (3–3.1 mM^{-1} cm^{-1}) extinction coefficients on one hand, and to the relatively high reaction rates observed especially at low ionic strength for the *P. denitrificans* couple, which approached the time resolution of the stopped-flow apparatus (dead time of 1.3 ms, determined by using the myoglobin-carbon monoxide combination reaction) on the other. Apparent second-order rate constants were determined from the slopes of the linear portions of the pseudo-first order plots (see "Results and Discussion"). Data fitting was performed by using either the Matlab (The MathWorks Inc.) or Scientist (Micromath Scientific Software Inc.) softwares. The standard deviation of the fitted parameters never exceeded 10%.

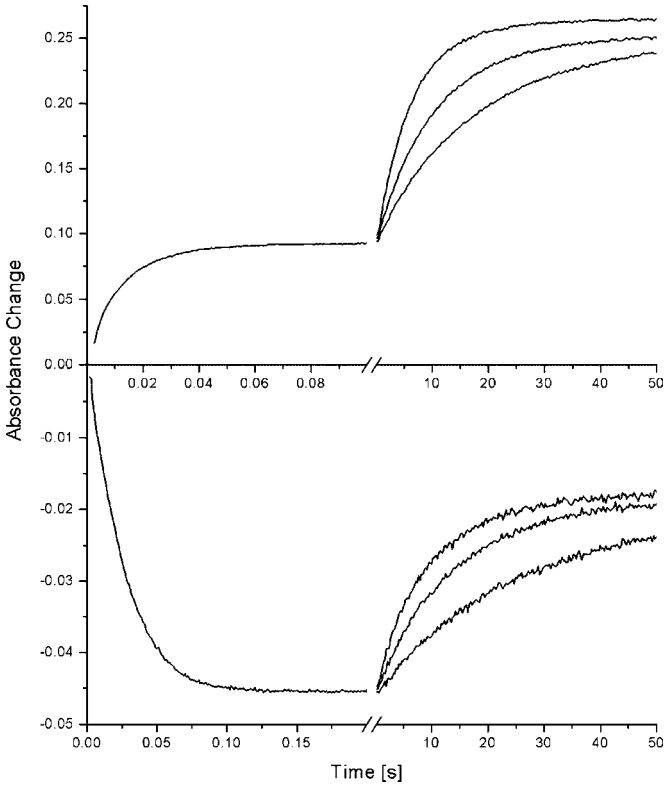

FIG. 1. **Ascorbate dependence of the forward and reverse ET reaction in the *Paracoccus* couple.** All protein samples were diluted in 20 mM Bis-Tris, pH 7.0, containing 50 mM KCl from concentrated stock solutions. *Top panel*, the reverse reaction in which oxidized Pd-c_{552} (32.7 μM) is mixed with ascorbate-reduced Pd-Cu_A (16.1 μM) in the stopped-flow apparatus. *Bottom panel*, the forward reaction in which ascorbate-reduced Pd-c_{552} (63.1 μM) is mixed with oxidized Pd-Cu_A (16.8 μM). In each *panel* note the split acquisition time base; the short time scale (*left*) represents the interprotein ET process between the two protein partners, and the long time scale (*right*) reports re-reduction by ascorbate (initially present at 0.25, 0.5, or 1 mM concentrations after mixing, from *bottom* to *top*, respectively) as followed at 551 nm. In the forward reaction the final equilibrium absorbance level is lower than the initial level because of complete reduction by ascorbate of Pd-Cu_A (and Pd-c_{552}), which does not absorb at this wavelength in the reduced state. Fitting of the observed time courses to a biexponential function yields the following results. In all cases the rate constant of the fast phase was independent of ascorbate concentration (forward reaction, k_{FAST} = 39.7 s^{-1}; reverse reaction, k_{FAST} = 83.3 s^{-1}). The fitted rate constants of the slow phase linearly depended on ascorbate concentration (forward reaction, k_{SLOW} = 0.041, 0.074, and 0.112 s^{-1}; reverse reaction, k_{SLOW} = 0.06, 0.1, and 0.16 s^{-1}, with ascorbate concentration varied as indicated above. In all cases the standard deviations of the fitted parameters were less than 2%). T = 8 °C.

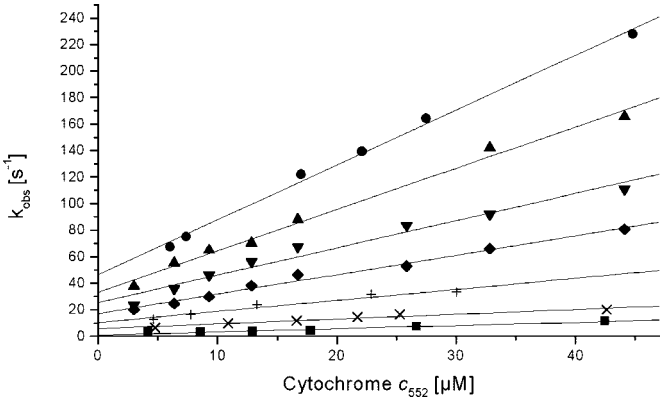

FIG. 2. **The forward physiological electron transfer reaction between *Paracoccus* cytochrome c_{552} and the Cu_A fragment.** The fast phase fitted rate constants of the ET reaction (see text and Fig. 1, *bottom panel*) between ferrous Pd-c_{552} and oxidized Pd-Cu_A (with concentrations ranging from 8.0 to 10.8 μM after mixing) at various ionic strength conditions (10 mM, ●; 15 mM, ▲; 25 mM, ▼; 35 mM, ♦; 50 mM, +; 100 mM, ×; 200 mM, ■) are plotted against the initial ferrous Pd-c_{552} concentration. Ascorbate concentration is 0.25 mM after mixing. *Solid lines* were calculated by linear regression of the data points. Other conditions were as in Fig. 1. T = 8 °C.

RESULTS AND DISCUSSION

In the present investigation the kinetics of electron transfer between two genetically engineered ET couples from a mesophilic and a thermophilic species have been studied by stopped-flow spectroscopy. The experimental rationale has been to prereduce one protein of each ET couple with the kinetically sluggish reductant ascorbate and to subsequently mix the proteins and follow the interprotein ET events at a suitable wavelength (see "Experimental Procedures"). At pH 7 the concentration of the true reductant, *i.e.* the ascorbate dianion, is very low (26, 27) and therefore not expected to interfere with the ET events taking place between the partners of interest. Fig. 1 depicts a typical example of the *Paracoccus* couple, studied in the forward, physiological direction (*bottom panel*, mixing of fully reduced Pd-c_{552} with oxidized Pd-Cu_A) and in the reverse direction (*top panel*, in which oxidized Pd-c_{552} is mixed with reduced Pd-Cu_A) followed at 551 nm, where the extinction of Pd-c_{552} is dominant. In either direction, absorbance changes take place on a short time scale (0.2 and 0.1 s) indicating partial oxidation (*bottom panel*) or reduction (*top panel*) of Pd-c_{552}. These experiments were carried out by varying the ascorbate concentration from 0.25 to 1 mM to exclude any competition of the reductant with the interprotein ET reaction of interest. Indeed as ascorbate concentration is increased, no significant change in rate or amplitude is observed on the short time scale, and all time courses display a simple exponential behavior. On longer time scales (50 s), however, the time-dependent absorbance changes appear to be linearly correlated to ascorbate concentration (not shown). These observations suggest that in the fast phase (Fig. 1, *left part* of *top* and *bottom panels*) interprotein ET occurs, taking the proteins to a transient equilibrium state controlled by the protein-chemical structural details and driven by the redox potential of the two ET proteins. On longer time scales (Fig. 1, *right part* of *top* and *bottom panels*) the ascorbate reaction takes the partially oxidized equilibrium ET couple mixture to the fully reduced state as expected from the larger driving force of ascorbate. Similar results were obtained with the *Thermus thermophilus* ET couple (not shown).

We have systematically studied the cytochrome c_{552} concentration dependence of the interprotein ET reaction with both couples as a function of ionic strength, using the ascorbate (0.25 mM after mixing) protocol described above. All observed fast phases could be fitted to a single exponential time course. The results of these experiments are shown in Figs. 2 and 3 (*P. denitrificans* couple) and Fig. 4 (*T. thermophilus* couple) in which the observed fitted rate constants are plotted as a function of cytochrome c_{552} concentration. The pseudo-first order plots were linear with respect to the varied cytochrome c_{552} concentration, although, especially at low cytochrome concentrations, there was some deviation from linear behavior. This is expected, because at low cytochrome c_{552} concentrations the reaction mixture is not under true pseudo-first order conditions. Nevertheless from the slope of the linear portion of the plots the apparent second-order rates for the interprotein ET reaction could be estimated and are given in Tables I and II for the *P. denitrificans* and *T. thermophilus* couple, respectively, at different ionic strength values. As can be seen from the reported data, the ET reaction of the *P. denitrificans* couple is strongly dependent on ionic strength with second-order rate constants ranging from ~4*10^6 to 9*10^4 M^{-1} s^{-1} and from

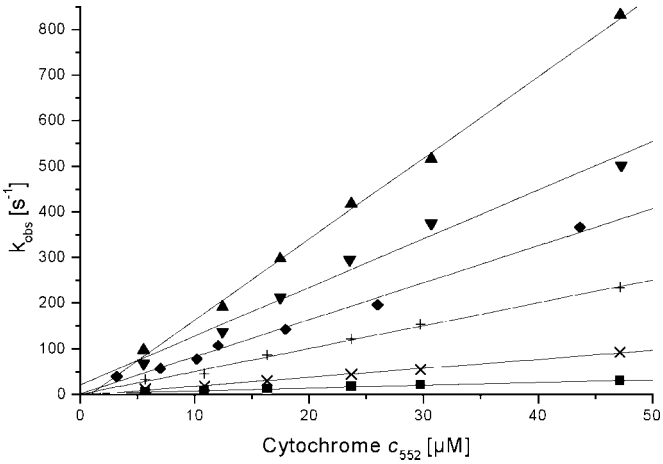

FIG. 3. **The reverse electron transfer reaction between *Paracoccus* cytochrome c_{552} and the Cu_A fragment.** The fast phase fitted rate constants of the ET reaction (see text and Fig. 1, *top panel*) between ferric Pd-c_{552} and reduced Pd-Cu_A (with concentrations in the range from 8.1 to 9.8 μM after mixing) at various ionic strength conditions (15 mM, ▲; 25 mM, ▼; 35 mM, ◆; 50 mM, +; 100 mM, ×; 200 mM, ■) are plotted against the initial ferric Pd-c_{552} concentration. Ascorbate concentration is 0.25 mM after mixing. *Solid lines* were determined by linear regression of the data points. Other conditions were as in Fig. 1. T = 8 °C.

$2*10^7$ to $6*10^5$ M^{-1} s^{-1}, for the forward and reverse ET reactions, respectively, as ionic strength is increased from 10 to 200 mM (see Table I). The apparent equilibrium constant for the physiological direction is thus about 0.2 for the *P. denitrificans* couple and does not appear to vary significantly with ionic strength. Although this result indicates a higher stability of reduced Pd-c_{552} over oxidized Pd-Cu_A, (i) this has also been observed previously (28) in the reaction between bovine heart cytochrome-*c* oxidase and yeast *iso*-1-cytochrome *c*, supporting our result; (ii) the reported redox potentials of the *P. denitrificans* couple are 270 and 240 mV for Pd-c_{552} and Pd-Cu_A, respectively (3, 29), which yields an equilibrium constant of about 0.3, in close agreement with our findings; and (iii) the ensuing exergonic ET reactions to the low spin heme *a* and the a_3-Cu_B center that account for O_2 reduction drive the thermodynamically unfavorable reaction in the physiological direction.

In contrast to these findings the ionic strength dependence of the *T. thermophilus* ET couple is very modest with rates in excess of 10^6 M^{-1} s^{-1} in either direction at the lowest ionic strength (see Fig. 4 and Table II). From these data an equilibrium constant of 4.8 was calculated for the *Thermus* protein pair, indicating that in this case the physiological direction is thermodynamically favored for the isolated domains. Several values of the redox potentials, depending strongly on the experimental conditions (temperature, ionic strength, pH), of the *Thermus* proteins have been reported (Th-Cu_A 240 mV up to 266 mV; see Refs. 4 and 30; Tt-c_{552} 200 mV (25) and 230 mV (31)), complicating the analysis and the comparison with the reported equilibrium constant gained from the kinetic data. However, calculation of the equilibrium constant with any of these values always confirms the physiological direction to be favored.

From the data shown in Figs. 2–4, as well as Tables I and II, Fig. 5 was constructed in which the logarithm of the apparent bimolecular rate constant is plotted as a function of the square root of ionic strength of the solution. As predicted by the Brønsted law (32), shown below in Equation 1, where k is the observed bimolecular rate constant at ionic strength I, k_0 the bimolecular rate constant at $I = 0$, B a term whose value, ~0.5 at 8 °C, is derived from Debye-Hückel equations, and z_A and z_B represent the ET-sensitive resident charges on the protein surfaces), the bimolecular rates in both directions decrease as the ionic strength is increased with slopes (the z_Az_B product) of about −4.6 for the *P. denitrificans* ET couple.

$$\log k = \log k_0 + 2Bz_Az_B\sqrt{I} \qquad \text{(Eq. 1)}$$

This indicates that two to three effective charges of opposite sign on each protein interface interact in the bimolecular electron transfer reaction, which is totally consistent with recent protein-protein docking calculations (33). The extrapolated rates at $I = 0$ ($k_0 = 1.2*10^7$ and $5.6*10^7$ M^{-1} s^{-1} for the forward and reverse reactions, respectively) indicate that the ET reactions approach the limit imposed by diffusion, as observed with wild-type aa_3 (13). Overall the results strongly suggest that the fragments approach each other and orient according to long-range electrostatic forces, showing the same principle of interaction as the native wild-type partners.

So far direct contacts between the two Pd-c552 and Pd-CuA are unclear. In a computational approach by Flöck and Helms (33), the complementarity of both protein surfaces were considered, followed by an energy minimization of the resulting complexes.

Using the minimal heme to Trp-121 (the electron entry site of Cu_A) distance as a further input parameter, two suggestions for an electron transfer complex resulted, clearly differing in the heme orientation. However, in both predicted complex structures, three ion pairs (involving three of the nine lysines on the cytochrome) could be identified. Consistently lysine 70 on the surface of the cytochrome was involved, and this residue also showed up in a recently performed chemical shift perturbation mapping experiment by NMR (34). Taken together, these data support the following scenario. In a very fast, diffusion-controlled process, electrostatic forces predominantly influence the formation of a loose encounter complex, allowing for some degree of freedom. Between two and three effective charges on each interaction protein surface provide the electrostatic setting for the initial attraction and steering of the two reaction partners. This is followed by a second step where the final (electron transfer) complex is generated mostly by specific, non-ionic contacts. A similar situation could be found for a cytochrome *f*-plastocyanin electron transfer couple from the cyanobacterium *Phormidium laminosum*, which has also been characterized by NMR (35) and double mutant cycle analysis by stopped-flow spectroscopy (36).

Fig. 5 also shows the ionic strength dependence of the *T. thermophilus* couple in the forward direction. The z_Az_B product (see Equation 1) is about −0.57 indicating that in the thermophilic couple the ET reaction is only slightly affected by electrostatic interactions. These results are in agreement with the surface properties of the high resolution x-ray structures of *P. denitrificans* aa_3 (37), *T. thermophilus* ba_3 (16), and of the corresponding structures of the substrate cytochrome partners (17, 38). Comparison of the possible interaction surfaces of both oxidases shows that of the conserved acidic residues of the aa_3 cytochrome-*c* oxidase proposed to be involved in cytochrome *c* binding (14, 15) only Asp-111 in the ba_3 oxidase from *Thermus* is present (16).

So far there is no direct experimental proof for the formation of a hydrophobically stabilized complex, but several lines of evidence support the notion that indeed mainly hydrophobic interactions govern the *Thermus* ET protein interaction. As ba_3 oxidase activity under turnover conditions is maximal at low ionic strength, Giuffrè *et al.* (19) exclude the formation of a high affinity electrostatically stabilized complex. In this system the cytochrome *c* off-rate could play a significant role and would be expected to limit the turnover rate as ionic strength is increased and as a hydrophobic complex is concomitantly stabilized. Our data presented here do not show any major depend-

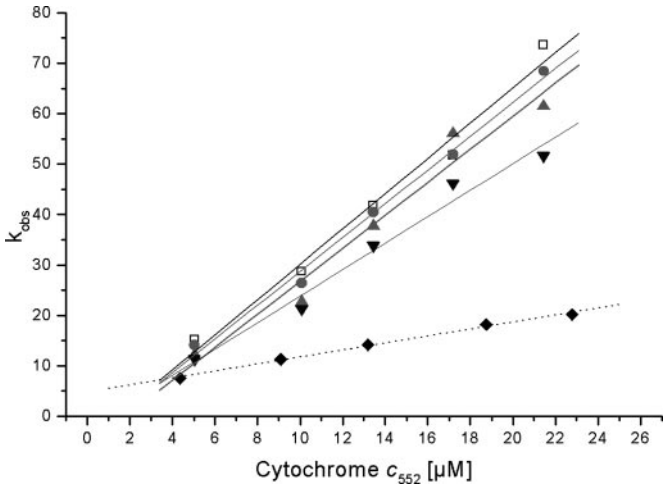

FIG. 4. **The electron transfer reaction between *Thermus* cytochrome c_{552} and the Cu_A fragment.** The fast phase fitted rate constants of the ET reaction between the Tt-c_{552} and Tt-Cu_A (forward direction, with concentrations in the range from 8.7 to 9.3 μM after mixing; reverse direction, 10.6 μM after mixing) couple are plotted as a function of the initial ferro- or ferri-Tt-c_{552} concentration. The forward direction was studied at the following ionic strength values: 15 mM (□); 25 mM (●); 50 mM (▲); and 100 mM (▼). The reverse reaction was only studied at an ionic strength of 25 mM (♦; *dotted line*). *Lines* were obtained by linear regression of the *data points*. Ascorbate concentration is 0.25 mM after mixing. Observation wavelength, 552 nm. Other conditions were as in Fig. 1. T = 8 °C.

ence on ionic strength, but it should be kept in mind that our experimental approach, in contrast to a turnover assay (19), only follows the initial steps of encounter and ET between the two proteins. Thus the fast kinetics observed here do not depend on a sluggish off-rate and therefore are only moderately affected by ionic strength (Fig. 5). We also note that the extrapolated second-order rate constant at I = 0 is already ~4*10^6 M^{-1} s^{-1} (see Fig. 5) at the temperature of the current experiments (8 °C) and is expected to further increase with temperature.

These considerations suggest that in contrast to the *Paracoccus* electron transfer couple, no electrostatically governed pre-orientation occurs within the *Thermus* protein couple. This is also supported by the electrostatic surface potentials, given in Fig. 6, indicating that opposite charges on the presumed interaction surfaces of the *Paracoccus* protein couple affect the ET process, whereas in the *Thermus* pair clearly hydrophobic amino acids dominate the interaction. Another confirmation for the different interaction modes of the two systems is the observation that the *Thermus* c_{552} is not a efficient substrate for the *P. denitrificans* cytochrome-*c* oxidase (39).

Fig. 7 depicts the temperature dependence of the ET reaction for the *Paracoccus* protein couple in the 8 to 26 °C range. In this temperature range the forward reaction displays a simple Arrhenius-like behavior with an activation energy of 44.4 kJ mol^{-1}. Analysis according to the Eyring equation (41) yields an activation enthalpy of 42.0 kJ mol^{-1} and an activation entropy of −59.5 J mol^{-1} K^{-1}. On the other hand, the reverse reaction is distinctly non-linear over this temperature range with a breakpoint at ~14 °C. Usually non-linear Arrhenius or Eyring plots arise from secondary reactions, which take place because of the deviation of activation parameters with rising temperature. Presently the most likely explanation is an intrinsic temperature-dependent conformational heterogeneity of the Cu_A domain in the reduced state, which differs from an unfolding process, because the rate constants in the 14 to 26 °C range are still quite high. Separate analysis of the two temperature ranges yield the following activation enthalpy and entropy parameters, respectively: 8 to 14 °C range, 39.6 kJ/mol and −63.4 J mol^{-1} K^{-1}; 14 to 26 °C range (*dashed line* in Fig. 7), 13.7 kJ/mol and −153.5 J mol^{-1} K^{-1}. Thus, in the low temperature range both the forward and reverse reactions display the same activation enthalpy (*i.e.* the same slope) and differ in the entropy of activation, as analysis according to the Eyring equation suggests. Therefore, and at least in the low temperature range, the rate is determined by translational, rotational, and vibrational or solvent entropic contributions rather than changes in the ground state reagent and product energy levels relative to the transition state.

All together the data indicate, again, that for this reaction the reverse direction is favored, although in the complete cytochrome-*c* oxidase heme *a* will serve as electron acceptor in a fast process, influencing the equilibrium between cytochrome *c* and Cu_A. By extrapolating the absolute bimolecular rate constant for the Pd-c_{552}-to-Cu_A electron transfer couple to 20 °C, one obtains a rate of 4.5*10^6 M^{-1} s^{-1}, and it is possible to compare this to previously reported rate constants for the reaction of the Cu_A domain with either cytochrome c_{550} from

TABLE I
Apparent second-order rate constants for the Paracoccus ET couple
N.D., not determined.

Ionic strength	$k_{forward}$	$k_{reverse}$	$k_{forward}/k_{reverse}$
mM	M^{-1} s^{-1}		
10	4.13·10^6	N.D.	N.D.
15	3.42·10^6	17.7·10^6	0.19
25	2.05·10^6	10.6·10^6	0.19
35	1.46·10^6	8.1·10^6	0.18
50	0.83·10^6	5.0·10^6	0.17
100	0.36·10^6	1.9·10^6	0.19
200	0.09·10^6	0.6·10^6	0.15

TABLE II
Apparent second-order rate constants for the Thermus ET couple
N.D., not determined.

Ionic strength	$k_{forward}$	$k_{reverse}$	$k_{forward}/k_{reverse}$
mM	M^{-1} s^{-1}		
15	3.50·10^6	N.D.	N.D.
25	3.35·10^6	0.7·10^6	4.8
50	3.27·10^6	N.D.	N.D.
100	2.62·10^6	N.D.	N.D.

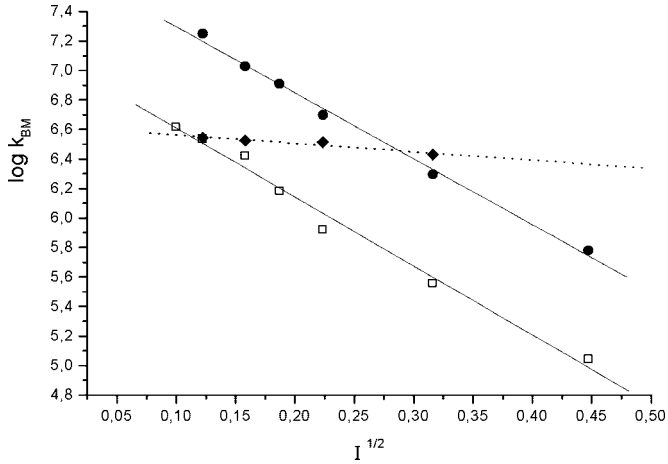

FIG. 5. **Ionic strength dependences of the apparent second-order ET rate constants.** The logarithm of the slopes, *i.e.* the apparent second-order ET rate constants (k_{BM}), of the data in Figs. 2–4 (see Tables I and II) are plotted *versus* the square root of ionic strength, varied by addition of KCl. □, *Paracoccus* forward reaction; ●, *Paracoccus* reverse reaction; ♦, *Thermus* forward reaction. The slope in this plot is the $z_A z_B$ product and represents the interacting charges on the protein interfaces. See text and Equation 1.

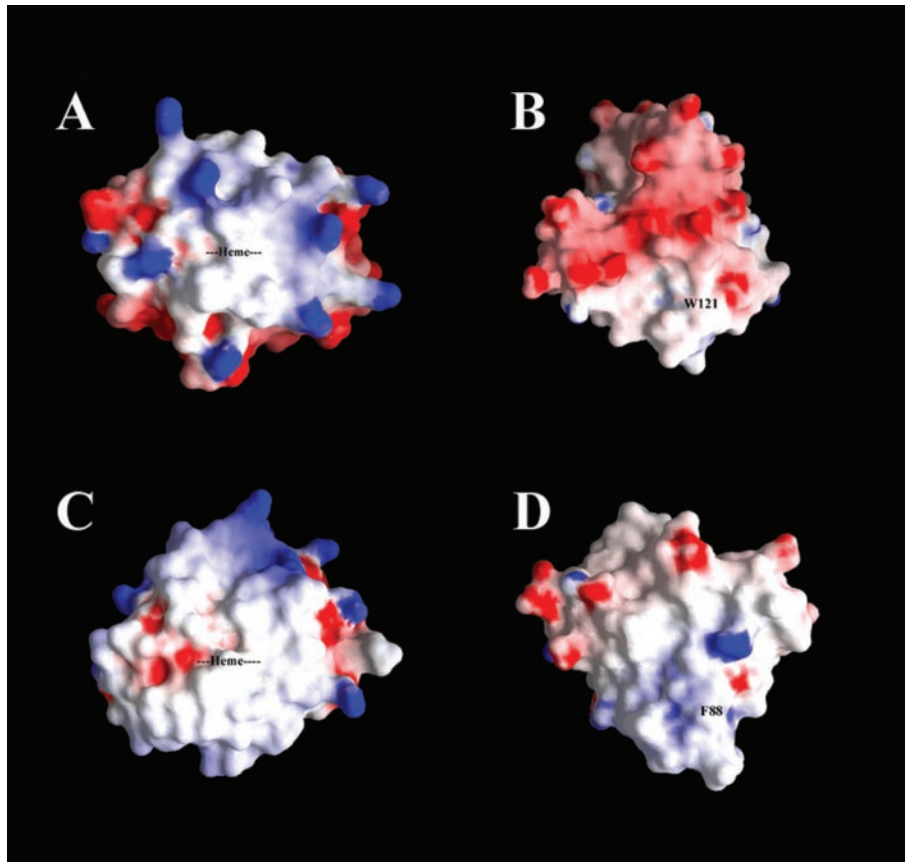

FIG. 6. **Electrostatic surface potentials for the *Paracoccus* and *Thermus* Cu_A domains and cytochromes c_{552}.** Electrostatic potentials of the proposed interaction surfaces for *P. denitrificans* cytochrome c_{552} (Protein Data Bank entry 1QL3) (*A*), *P. denitrificans* Cu_A fragment (Protein Data Bank entry 1AR1) (*B*), *T. thermophilus* c_{552} (Protein Data Bank entry 1C52) (*C*), and *T. thermophilus* Cu_A (Protein Data Bank entry 1EHK) (*D*) are shown. Coloring is according to the calculated electrostatic potential with GRASP (40) with boundary values from −15 kT (*intense red*) to +15 kT (*intense blue*) for the Cu_A proteins and from −5 to +5 kT for the cytochromes. The approximate location of the partially solvent exposed heme cofactors is shown in *black text*. The Cu_A site is positioned *under* the protein surface within 5 Å from Trp-121, the electron entry site in *P. denitrificans* cytochrome-*c* oxidase (14, 15, 41); in the Tt-Cu_A protein Phe-88 has been suggested to be the corresponding residue (16–18). Both residues are *highlighted* in *black text*.

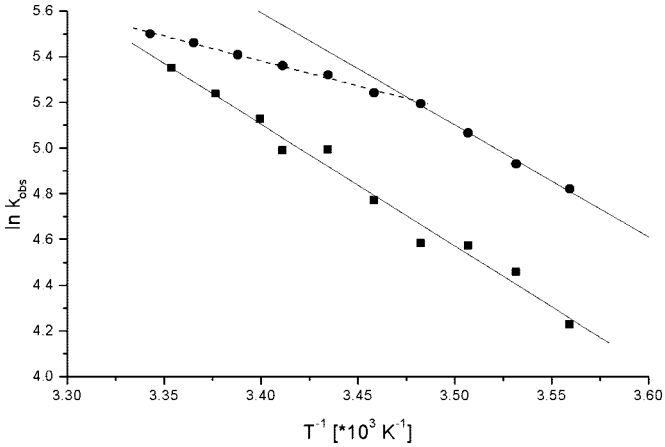

FIG. 7. **The temperature dependence of the ET reaction between *Paracoccus* fragments.** The natural logarithm of the observed rate constants is plotted *versus* the reciprocal absolute temperature (varied from 8 to 26 °C). ■, forward reaction (Pd-c_{552} = 6 μM, Pd-Cu_A = 10.8 μM after mixing); ●, reverse reaction (Pd-c_{552} = 5 μM, Pd-Cu_A = 10.7 μM after mixing). Experiments were performed in 20 mM Bis-Tris, pH 7.0, containing 10 mM KCl. *Solid* or *dashed lines* are the best fits obtained by analysis according to the Eyring equation (42). See text for details on the activation parameters.

P. denitrificans or horse heart cytochrome *c* (8). This analysis shows that the reaction with Pd-c_{552} is about 3-fold faster than the reaction with Pd-c_{550} ($1.46*10^6$ $M^{-1}s^{-1}$) and 15-fold faster than the reaction with horse heart cytochrome *c* ($3*10^5$ $M^{-1}s^{-1}$). This observation provides an independent kinetic argument that the c_{552} protein is the favored electron donor for the aa_3 cytochrome-*c* oxidase from *P. denitrificans*. This is also supported by the fact that a supercomplex of bc_1 complex, cytochrome c_{552}, and aa_3 cytochrome oxidase can be found in *Paracoccus* membranes (10). Considering that the native cytochrome c_{552} has a membrane anchoring domain and an additional charged domain, it should be pointed out that these structural elements could further stabilize a supercomplex and may even allow higher electron transfer rates, without the constraints imposed by three-dimensional diffusion of the electron mediator.

Finally, the results presented in this investigation show that the kinetic processes taking place between the engineered proteins are truly bimolecular, *i.e.* with every collisional encounter resulting in a very efficient ET process. One may also assume that additional structural determinants present in the full-size proteins (complexes) may further modulate the specificity and efficiency of the interaction of oxidases with their substrates. All together the present study shows that the protein fragments studied are very good models of the initial ET events in oxidases without the complication of the ensuing ET processes taking place within the oxidases.

Acknowledgments—We thank Maurizio Brunori for hospitality and for access to the stopped-flow apparatus, David Waugh for providing the plasmid pRK603, Christian Lücke for help in preparing Fig. 6, Oliver-Matthias H. Richter for critical reading of the manuscript, Hans-Werner Müller for excellent technical assistance, and a number of colleagues for helpful discussions on the *P. denitrificans* Cu_A fragment metal insertion.

REFERENCES

1. Drosou, V., Reincke, B., Schneider, M., and Ludwig, B. (2002) *Biochemistry* **41,** 10629–10634
2. Schultz, B. E., and Chan, S. I. (2001) *Annu. Rev. Biophys. Biomol. Struct.* **30,** 23–65
3. Lappalainen, P., Aasa, R., Malmström, B. G., and Saraste, M. (1993) *J. Biol. Chem.* **268,** 26416–26421
4. Slutter, C. E., Sanders, D., Wittung, P., Malmström, B. G., Aasa, R., Richards, J. H., Gray, H. B., and Fee, J. A. (1996) *Biochemistry* **35,** 3387–3395
5. Salgado, J., Warmerdam, G., Bubacco, L., and Canters, G. W. (1998) *Biochemistry* **37,** 7378–7389
6. von Wachenfeldt, C., de Vries, S., and van der Oost, J. (1994) *FEBS Lett.* **340,** 109–113
7. Baker, S. C., Ferguson, S. J., Ludwig, B., Page, M. D., Richter, O. M. H., and van Spanning, R. J. (1998) *Microbiol. Mol. Biol. Rev.* **62,** 1046–1078

8. Lappalainen, P., Watmough, N. J., Greenwood, C., and Saraste, M. (1995) *Biochemistry* **34,** 5824–5830
9. Turba, A., Jetzek, M., and Ludwig, B. (1995) *Eur. J. Biochem.* **231,** 259–265
10. Berry, E. A., and Trumpower, B. L. (1985) *J. Biol. Chem.* **260,** 2458–2467
11. Turba, A. (1993) *Molekularbiologische und biochemische Charakterisierung des Membran-gebundenen Cytochrom c_{552} aus Paracoccus denitrificans*, Ph.D. thesis, University of Frankfurt, Frankfurt, Germany
12. Dethmers, J. K., Ferguson-Miller, S., and Margoliash, E. (1979) *J. Biol. Chem.* **254,** 11973–11981
13. Antalis, T. M., and Palmer, G. (1982) *J. Biol. Chem.* **257,** 6194–6206
14. Witt, H., Malatesta, F., Nicoletti, F., Brunori, M., and Ludwig, B. (1998) *Eur. J. Biochem.* **251,** 367–373
15. Drosou, V., Malatesta, F., and Ludwig, B. (2002) *Eur. J. Biochem.* **269,** 2980–2988
16. Soulimane, T., Buse, G., Bourenkov, G. P., Bartunik, H. D., Huber, R., and Than, M. E. (2000) *EMBO J.* **19,** 1766–1776
17. Than, M. E., Hof, P., Huber, R., Bourenkov, G. P., Bartunik, H. D., Buse, G., and Soulimane, T. (1997) *J. Mol. Biol.* **271,** 629–644
18. Soulimane, T., von Walter, M., Hof, P., Than, M. E., Huber, R., and Buse, G. (1997) *Biochem. Biophys. Res. Commun.* **237,** 572–576
19. Giuffrè, A., Forte, E., Antonini, G., D'Itri, E., Brunori, M., Soulimane, T., and Buse, G. (1999) *Biochemistry* **38,** 1057–1065
20. Steinrücke, P., Steffens, G. C., Panskus, G., Buse, G., and Ludwig, B. (1987) *Eur. J. Biochem.* **167,** 431–439
21. Kapust, R. B., and Waugh, D. S. (2000) *Protein Expr. Purif.* **19,** 312–318
22. Wingfield, P. T. (1998) in *Current Protocols in Protein Science* (Coligan, J. E., Dunn, B. M., Ploegh, H. L., Speicher, D. W., and Wingfield, P. T., eds) John Wiley & Sons, Inc., New York
23. Reincke, B., Thöny-Meyer, L., Dannehl, C., Odenwald, A., Aidim, M., Witt, H., Rüterjans, H., and Ludwig, B. (1999) *Biochim. Biophys. Acta* **1411,** 114–120
24. Arslan, E., Schulz, H., Zufferey, R., Künzler, P., and Thöny-Meyer, L. (1998) *Biochem. Biophys. Res. Commun.* **251,** 744–747
25. Fee, J. A., Chen, Y., Todaro, T. R., Bren, K. L., Patel, K. M., Hill, M. G., Gomez-Moran, E., Loehr, T. M., Ai, J., Thöny-Meyer, L., Williams, P. A., Stura, E., Sridhar, V., and McRee, D. E. (2000) *Protein Sci.* **9,** 2074–2084
26. Al Ayash, A. I., and Wilson, M. T. (1979) *Biochem. J.* **177,** 641–648
27. Myer, Y. P., Thallam, K. K., and Pande, A. (1980) *J. Biol. Chem.* **255,** 9666–9673
28. Szundi, I., Cappuccio, J. A., Borovok, N., Kotlyar, A. B., and Einarsdottir, O. (2001) *Biochemistry* **40,** 2186–2193
29. Schneider, M. (2000) *Zielgerichtete Mutagenese am Cytochrom C_{552} aus Paracoccus denitrificans*, Diploma thesis, University of Frankfurt, Frankfurt, Germany
30. Inmoos, C., Hill, M. G., Sanders, D., Fee, J. A., Slutter, C. E., Richards, J. H., and Gray, H. B. (1996) *J. Biol. Inorg. Chem.* **1,** 529–531
31. Hon-Nami, K., and Oshima, T. (1977) *J. Biochem. (Tokyo)* **82,** 769–776
32. Brønsted, J. N., and La Mer, V. K. (1924), *J. Am. Chem. Soc.* **46,** 555–573
33. Flöck, D., and Helms, V. (2002) *Proteins Struct. Funct. Genet.* **47,** 75–85
34. Wienk, H., Maneg, O., Lücke, C., Pristovšek, P., Löhr, F., Ludwig, B., and Rüterjans, H. (2003) *Biochemistry* **42,** 6005–6012
35. Crowley, P. B., Otting, G., Schlarb-Ridley, B. G., Canters, G. W., and Ubbink, M. (2001) *J. Am. Chem. Soc.* **123,** 10444–10453
36. Hart, S. E., Schlarb-Ridley, B. G., Delon, C., Bendall, D. S., and Howe, C. J. (2003) *Biochemistry* **42,** 4829–4836
37. Iwata, S., Ostermeier, C., Ludwig, B., and Michel, H. (1995) *Nature* **376,** 660–669
38. Harrenga, A., Reincke, B., Rüterjans, H., Ludwig, B., and Michel, H. (2000) *J. Mol. Biol.* **295,** 667–678
39. Drosou, V. (2002) *Cytochrom c als Elektronendonor für die aa_3-Oxidase aus Paracoccus denitrificans*, Ph.D. thesis, University of Frankfurt, Frankfurt, Germany
40. Nicholls, A., Sharp, K. A., and Honig, B. (1991) *Proteins* **11,** 281–296
41. Witt, H., Malatesta, F., Nicoletti, F., Brunori, M., and Ludwig, B. (1998) *J. Biol. Chem.* **273,** 5132–5136
42. Atkins, P. W. (1990) *Physical Chemistry*, 4th Ed., p. 851, Oxford University Press, Oxford

Different Interaction Modes of Two Cytochrome-*c* Oxidase Soluble Cu_A Fragments with Their Substrates

Oliver Maneg, Bernd Ludwig and Francesco Malatesta

J. Biol. Chem. 2003, 278:46734-46740.
doi: 10.1074/jbc.M307594200 originally published online August 23, 2003